Zeeman Effect

Marnik Metting van Rijn

February 9, 2020

Abstract

The impact of a magnetic field on the light emission of a neon lamp was studied by observing the spectral lines using a Lummer interferometer. The elementary charge mass ratio was calculated to be $(1.9 \pm 0.1) \cdot 10^{11}$ C/kg, where literature values deviate by 8 %.

Contents

1 Introduction

The Zeeman effect describes the splitting of spectral lines if a magnetic field is applied to the light emitted by a radiant body [1]. It was first observed by P. Zeeman in Leiden in 1896 and three years after partially explained by Hendrik Antoon Lorentz [2]. They were awarded the Nobel Prize in Physics in 1902 ≪recognition of the extraordinary service they rendered by their researches into the influence of magnetism upon radiation phenomena≫[4].

In this experiment the spectral lines of a neon lamp is observed using a Lummer interferometer. The Zeeman effect can then be illustrated by applying a magnetic field and observing the splitting of the spectral lines in different intensities [2].

2 Theory

2.1 The Lorentz Theory

The Lorentz theory is based on the model of a harmonically oscillating charge, which emits radiation of the frequency corresponding to the ground state. The harmonic oscillation is driven by an electric field which is described in the following equation of motion:

$$\ddot{x}_i + \omega_0^2 x_i = \frac{e}{m_e}(\dot{x} \wedge H)_i, \tag{1}$$

where $i = 1, 2, 3$ and $\boldsymbol{H}$ denotes the magnetic field. Provided that the magnetic field $\boldsymbol{H} = (0, 0, H)$ it follows that the parallel component to the oscillation is not affected. This can be solved to

$$x_1 = cos[\omega_0 + \Omega)t]$$
$$x_1 = -sin[\omega_0 + \Omega)t]$$

and

$$x_2 = cos[\omega_0 - \Omega)t]$$
$$x_2 = sin[\omega_0 - \Omega)t],$$

where a profound derivation can be found in [2]. The factor Ω is defined as

$$\Omega := \frac{eH}{2m_e}, \tag{2}$$

where m_e corresponds to the mass of the electron. Considering that the magnetic field points in z-direction the solution found for Equation (1) describe a left circular wave (x_1, y_1) and a right circular wave (x_2, y_2). Equation (2) provides a possibility to determine the absolute value of e and the sign of e/m_e.

Equation (1) describes a radiating particle with no restriction to its frequency. This does not coincide with the discreetness of energy levels in quantum mechanics. It contradicts energy conservation as the electron is accelerated and therefore emits radiation whereas the solution of Equation (1) show no decrease in energy. Further the quantisation of angular momentum and the concept of spin are neglected in the model.

2.2 The Bohr Model

Bohr postulated that electrons only radiate during a transition from a discreet energy level to another. From a quantum mechanical view the energy is discrete in integer multiple n of the Planck's constant h. Further the orbital angular momentum $\boldsymbol{L}$ is analogously only possible in integer multiple l of the reduced Planck's constant $\hbar$.

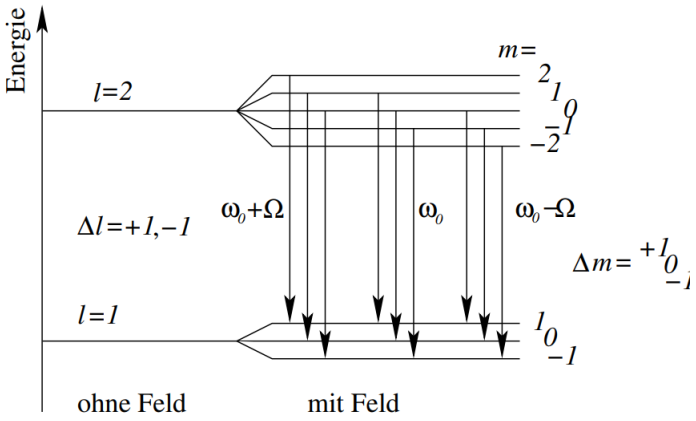

Figure 1: For fixed quantum number n the quantum number l and m are considered for the transitions described in Section 2.3. The precession frequency Ω is responsible for the change in quantum number m. The left side corresponds to the situation where no magnetic field is applied, whereas on the right a magnetic field acts on the radiant body. Illustration from [2].

The magnetic moment $\boldsymbol{\mu}$ of an electron orbiting is defined as

$$\boldsymbol{\mu} = -\frac{e}{2m_e}\boldsymbol{L}, \tag{3}$$

where $\boldsymbol{L}$ is the orbital angular momentum. The torque is defined as

$$\boldsymbol{\tau} = \boldsymbol{\mu} \wedge \boldsymbol{H}, \tag{4}$$

which leads to the equation of motion

$$\boldsymbol{\tau} = \dot{\boldsymbol{L}} \tag{5}$$

by inserting Equation (3) in Equation (4). Solving the equation of motion yields a precession in the components perpendicular to $\boldsymbol{H}$. The precession frequency is

$$\Omega = \frac{eH}{2m_e} \tag{6}$$

and is called Larmor frequency.

2.3 Selection Rules

Bohr's second postulate states that a photon is emitted if an electron descends to a lower state (see [3] for further information). In this experiment only several transitions are of importance as other transitions have a negligible possibility to occur. These include transitions where

- Δl $= \pm 1$ and
- Δm $= \pm 1$ or 0.

The frequency variation Ω shown in Figure 1 can be determined by the magnetic energy:

$$\hbar\Omega = \Delta E_m^{upper} - \Delta E_m^{lower} = \hbar\frac{eH}{2m_e}(m^{upper} - m^{lower}) = \hbar\frac{eH}{2m_e}\Delta m.$$

Considering the selection rules introduced previously Ω is

$$\Omega = \pm\frac{eH}{2m_e} \quad \text{or} \quad 0 \tag{7}$$

which coincides with the Larmor frequency.

2.4 Spin

A more general model of the Zeeman effect includes the consideration of spin, which is further of discreet nature. In the Stern-Gerlach experiment the magnetic torque μ_S of the spin S was found to be [5]

$$\mu_S = \frac{e\hbar}{2m_e} = -\frac{e}{m_e}S. \tag{8}$$

For electrons the quantum number s corresponding to the spin S takes the values -1/2 and 1/2. They are related by the definition $S = s \cdot \hbar$. Further the total angular momentum number j is defined by $j = l \pm s$ which can be determined using the operator $J^2 = \hbar^2 j(j+1)$. For electrons the spin quantum number m_s equals $\pm 1/2$, which can further be added to the $2l+1$ quantum number m_l. This results in a new quantum number $m_j = m_l + m_s$ which lies within $-j, -j+1, ..., j-1, j$.

2.5 Many-Electron Atoms

For atoms with multiple electrons the total angular momentum can be summed together to define the total orbital angular momentum

$$L = \sum_i l_i \tag{9}$$

and analogously the total spin

$$S = \sum_i s_i, \tag{10}$$

where i counts the number of electrons in the atom. These quantity can then be combined to define the total angular momentum

$$J = L + S, \tag{11}$$

which is known as $LS - coupling$. This quantitatively describes the effect of the magnetic field of the nucleus on the spin of the electron which has a relative velocity in respect to the nucleus. Another effect is due to the coupling of the total angular momentum to the spin, which is often found for heavier atoms [5]. Therefore, the total angular momentum is defined as

$$J = \sum_i (l_i + s_i), \tag{12}$$

where i sums over the number of electrons in the atom. Equation (12) is known as $jj - coupling$. The quantum numbers introduced above yield further transition rules, which are

- $\Delta S = 0$,
- $\Delta L = 0$ or $\pm$ 1 and
- $\Delta J = 0$ or $\pm$ 1.

2.6 Singlet and Triplet Structure of the First Excited State of the Helium Atom

Helium is an atom with two electrons and therefore the simplest many-electron atom. The Pauli exclusion principle states that the wavefunctions of two identical fermions must be antisymmetric with respect to the exchange operator. The state of the electrons consists of a spatial part and a spin part, which is either

$$\chi_- = \frac{1}{\sqrt{2}}(\chi_{\uparrow 1 \downarrow 2} - \chi_{\downarrow 1 \uparrow 2}) \tag{13}$$

for antisymmetric spin and

$$\chi_+ = \frac{1}{\sqrt{2}}(\chi_{\uparrow 1 \downarrow 2} + \chi_{\downarrow 1 \uparrow 2}), \tag{14}$$

$$\chi_{\uparrow 1 \uparrow 2} \quad \text{or} \quad \chi_{\downarrow 1 \downarrow 2} \tag{15}$$

for symmetric spin. The ground spatial function is ψ_1, whereas ψ_2 defines the first excited spatial function. Therefore, the allowed states are of the following form:

$$\frac{1}{\sqrt{2}}[\psi_1(\boldsymbol{r}_1)\psi_2(\boldsymbol{r}_2) + \psi_1(\boldsymbol{r}_2)\psi_2(\boldsymbol{r}_1)]\chi_- \tag{16}$$

$$\frac{1}{\sqrt{2}}[\psi_1(\boldsymbol{r}_1)\psi_2(\boldsymbol{r}_2) - \psi_1(\boldsymbol{r}_2)\psi_2(\boldsymbol{r}_1)]\chi_+ \tag{17}$$

$$\frac{1}{\sqrt{2}}[\psi_1(\boldsymbol{r}_1)\psi_2(\boldsymbol{r}_2) - \psi_1(\boldsymbol{r}_2)\psi_2(\boldsymbol{r}_1)]\chi_{\uparrow 1 \uparrow 2} \tag{18}$$

$$\frac{1}{\sqrt{2}}[\psi_1(\boldsymbol{r}_1)\psi_2(\boldsymbol{r}_2) - \psi_1(\boldsymbol{r}_2)\psi_2(\boldsymbol{r}_1)]\chi_{\downarrow 1 \downarrow 2}. \tag{19}$$

$$\tag{20}$$

As Equation (16) is the only form, where the spin part is antisymmetric, this defines a singlet structure. Following the three residual forms define a triplet structure.

2.7 Calculation of the g-Factor

In [2] following definition is given for the case of LS-coupling:

$$\boldsymbol{\mu_j} = -\frac{e}{2m_e} g \boldsymbol{J}. \tag{21}$$

Further the absolute values for $\boldsymbol{J}$, $\boldsymbol{L}$ and $\mathbf{S}$ are given by $\sqrt{J(J+1)}$, $\sqrt{L(L+1)}$ and $\sqrt{S(S+1)}$, which are needed to solve Equation (21) for g. Knowing that $\mu_j = \mu_l + \mu_s$ and using Equation (3) and Equation (8) it follows that

$$-\frac{e}{2m_e} g \boldsymbol{J} = -\frac{e}{m_e}\boldsymbol{S} - \frac{e}{2m_e}\boldsymbol{L}. \tag{22}$$

Taking the absolute values and solving for g yields

$$g = 1 + \frac{J(J+1) + S(S+1) - L(L+1)}{2J(J+1)}. \tag{23}$$

2.8 Derivation of the Equation of Motion Using Lagrangian Mechanics

The Lagrangian of an electron in a magnetic field is given by

$$L = \frac{1}{2} m \dot{\boldsymbol{r}}^2 - e\phi + e\dot{\boldsymbol{r}} \cdot \boldsymbol{A}. \tag{24}$$

Using the Euler-Lagrange equations

$$\sum_i \frac{\partial L}{\partial q_i} - \frac{d}{dt}\frac{\partial L}{\partial \dot{q}_i} = 0, \tag{25}$$

where i sums over all spatial coordinates, the equation of motion for an electron in a magnetic field is given by

$$m\ddot{r}_i + e\frac{dA_i}{dt} = -e\frac{\partial \phi}{\partial r_i} + e\sum_j \dot{r}_j \frac{\partial A_j}{\partial r_i}. \tag{26}$$

The total time derivative of the vector potential $\boldsymbol{A}$ is given by

$$\frac{dA_i}{dt} = \frac{\partial A_i}{\partial t} + \sum_j \dot{r}_j \frac{\partial A_i}{\partial r_j}. \tag{27}$$

Finally Equation (27) can be inserted in Equation (26) which results in

$$m\ddot{r}_i = e[-\frac{\partial A_i}{\partial t} - \frac{\partial \phi}{\partial r_i}] + e\sum_j [\dot{r}_j \frac{\partial A_j}{\partial r_i} - \dot{r}_j \frac{\partial A_i}{\partial r_j}] \tag{28}$$

and coincides with Equation (1).

2.9 Solving the Schrödinger Equation for an Electron in a Magnetic Field

Using a Legendre transformation Equation (24) can be used to find the Hamiltonian of the problem

$$H = -\frac{\hbar^2}{2m}\Delta + \frac{e\hbar}{imc}\boldsymbol{A}\cdot\boldsymbol{\nabla} - eV. \tag{29}$$

The Hamiltonian H can be separated in two parts

$$H_0 = -\frac{\hbar^2}{2m}\Delta - eV \quad \text{and} \tag{30}$$

$$H_1 = \frac{e\hbar}{imc}\boldsymbol{A}\cdot\boldsymbol{\nabla}. \tag{31}$$

In order to measure H_0 and H_1 simultaneously, the commutator $[H_0, H_1]$ must vanish for any wavefunction Ψ.

$$H_0H_1\Psi = -\frac{e\hbar^3}{2im^2c}(\partial_j^2 A_i)\partial_i\Psi - \frac{e\hbar^3}{2im^2c}A_i\partial_i\partial_j^2\Psi - \frac{e^2V\hbar}{imc}A_i\partial_i\Psi \tag{32}$$

$$H_1H_0\Psi = -\frac{e\hbar^3}{2im^2c}A_i\partial_j^2\partial_i\Psi - \frac{e^2V\hbar}{imc}A_i\partial_i\Psi \tag{33}$$

In Equation (32) and Equation (33) the Einstein sum convention and the definition $\partial_i = \frac{\partial}{\partial r_i}$ is used. Assuming that $\boldsymbol{\nabla}\cdot\boldsymbol{A} = 0$ it follows that $\Delta A = 0$ using the identity $\Delta\Phi = \nabla(\nabla\cdot\Phi) - \nabla\wedge(\nabla\wedge\Phi)$ and Maxwell's equation for stationary conditions. Therefore the commutator vanishes for any wavefunction Ψ and H_0 and H_1 can be measured simultaneously. In [2] a derivation is provided that the total energy of the Hamiltonian H is

$$E_n = E_n^0 + \frac{eH}{2m_ec}\hbar m. \tag{34}$$

3 Experimental Setup and Measurement Procedures

In this experiment the light of a neon tube is analysed using a Lummer interferometer, where an overview of the setup is shown in Figure 2. The interferometer provides a possibility to determine the wavelengths difference of the emitted photons from the neon light. A schematic of a Lummer interferometer is shown in Figure 3. The incident light D' penetrates perpendicularly into a wedge shaped plate and reflects at point D. Assuming either that the angle β is large or the index of refraction n of the Lummer plate is large, the incident light will be reflected almost totally. The beam will then propagate along the plate while emitting part of its beam every time it gets reflected. The phase difference ϕ of the rays exiting the Lummer plate is given by

$$\phi = \frac{4\pi d}{\lambda}\sqrt{n^2 - sin^2\alpha}, \tag{35}$$

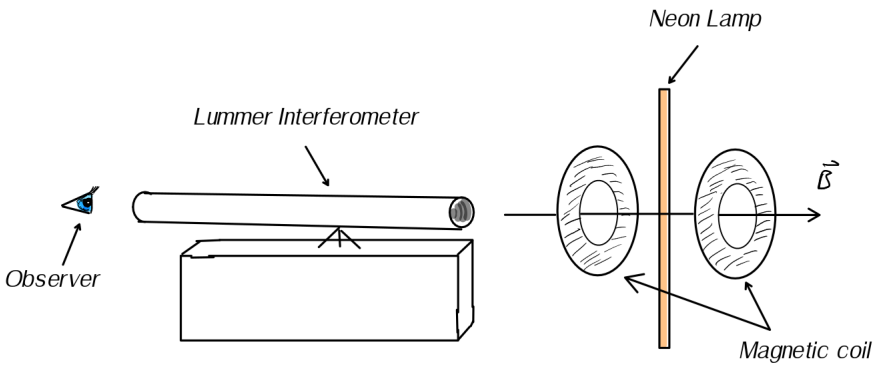

Figure 2: Experimental setup used to observe the zeeman effect.

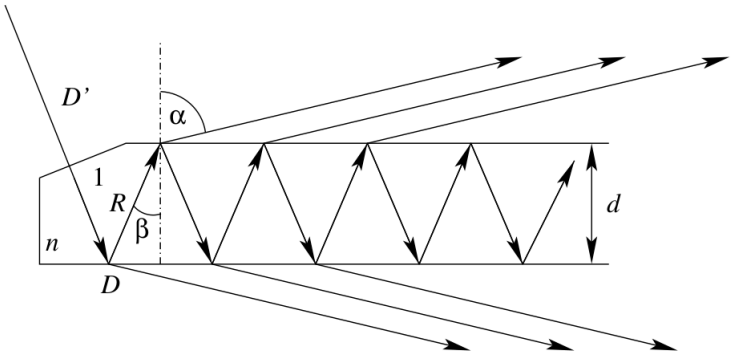

Figure 3: Schematic of a Lummer interferometer from [2].

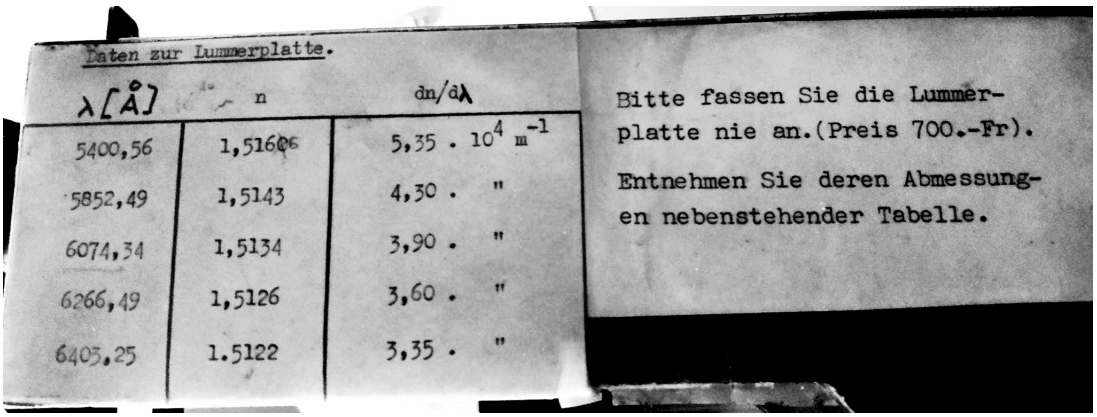

Figure 4: Characteristics of the interferometer used in this experiment.

where d, α, β and n are defined corresponding to Figure 3 and λ the wavelength of the incoming beam [2]. Imposing the condition for constructive interference $\phi = 2\pi z$, where z is an integer, Equation 35 can be rewritten as

$$z = \frac{2d}{\lambda}\sqrt{n^2 - sin^2\alpha}. \tag{36}$$

For a fix z, the splitting of one beam $\frac{d\lambda}{d\alpha}$ is given by

$$\lambda(\alpha) = \frac{2d}{z}\sqrt{n^2(\lambda(\alpha)) - sin^2\alpha}, \tag{37}$$

which is an implicit representation [2] of

$$\frac{d\lambda}{d\alpha} = -\frac{\frac{\partial F}{\partial \alpha}}{\frac{\partial F}{\partial \lambda}}. \tag{38}$$

The function F is given by

$$F(\alpha, \lambda) = \lambda - \frac{2d}{z}\sqrt{n^2(\lambda) - sin^2\alpha}, \tag{39}$$

which can be used to solve for $\frac{d\lambda}{d\alpha}$. Therefore in the dispersion region the change in wavelength for different angles α is given by

$$\Delta\lambda \approx |\frac{\lambda^2\sqrt{n^2-1}}{2d(n^2 - 1 - n\lambda\frac{dn}{d\lambda}}|, \tag{40}$$

where $\alpha \approx \frac{\pi}{2}$ and $sin\alpha \approx 1$ was assumed [2]. Equation (40) bears a possibility to measure the change in wavelength $\Delta\lambda$ by observing the change in interference pattern $\Delta\alpha$. In this experiment, the wavelength is changed until the interference lines are equally spaced which is only the case when the variation in wavelength is $\Delta\lambda$ [2].

The values for n and $dn/d\lambda$ can be taken from Figure 4 and the thickness of the plate is $d = 3.18$ mm.

Figure 2 shows two coils inducing a magnetic field through the neon lamp, where the magnitude can be adjusted by changing the current flow through the coils. The magnitude of the field as a function of the current is shown in Figure 5, where a fit is provided for calculations.

As derived in Section 2.3 the degeneracy of the energy levels splits if a magnetic field is applied. Using a knob the magnetic field is adjusted until the current is found where the interference lines are equidistant. The difference in energy ΔE between two σ-polarized multiplets is defined as

$$\Delta E = \frac{e\hbar}{2m_e} H f(g_1, g_2), \tag{41}$$

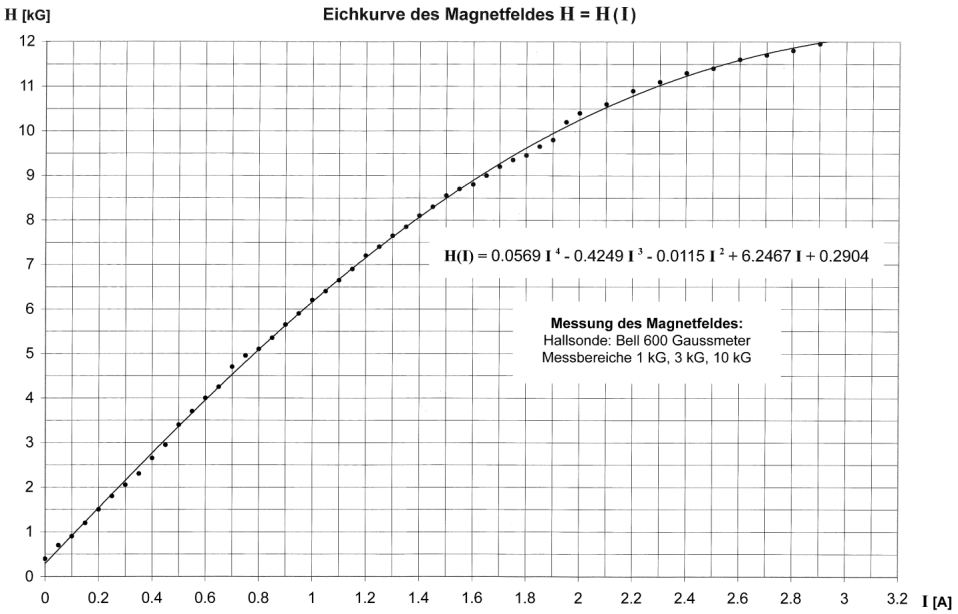

Figure 5: The magnitude of the magnetic field as a function of the current.

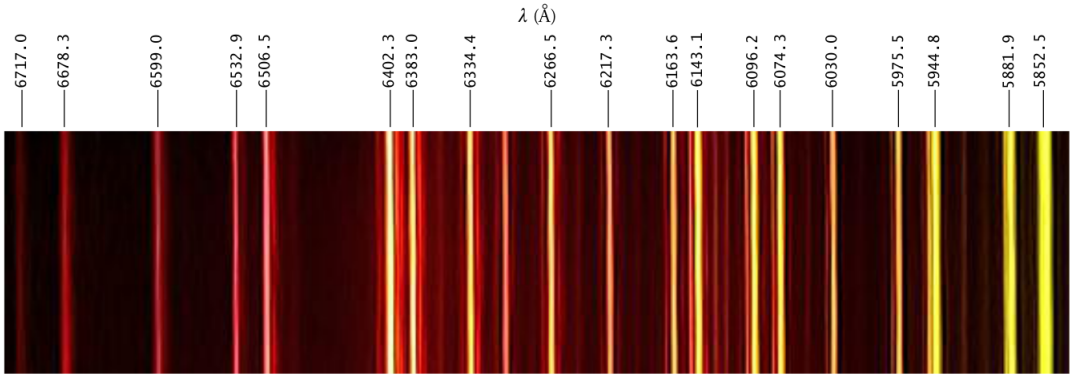

Figure 6: Spectral lines of a neon lamp with corresponding wavelenght [2].

which is derived in [2]. The function $f(g_1, g_2)$ is a function of the g-factors which are discussed in Section 2.7. If the lines are equally spaced, the energy ΔE is equal to $\Delta\epsilon$ which is defined as the energy difference between two maxima of the lines. As derived in [2] a further possibility is to use $\Delta\epsilon/2$ which would correspond to half a wavelength shift and half the current.

4 Data and Analysis

Using the interferometer five spectral lines were identified and are shown in Table 1. This was done by observing the colour of the spectral lines and comparing to Figure 6.
For each spectral line the current was then adjusted until the pattern got equidistant. Figure 7 shows the equidistant pattern observed through the Lummer interferometer for a wavelength of 603 nm. Finding this pattern was rather difficult and, therefore, an error of 0.1 A for the current had to be taken into account. The error was then propagated in accordance with linear error propagation theory, where *uncertainties* [6] was used. Using the fit shown in Figure 5 the magnetic field was then calculated and is shown in Table 1. As the wavelength is known, the values for J_1, J_2, g_1, g_2 and, therefore, $f(g_1, g_2)$ can be taken from [2]. Further the following relation holds for the elementary

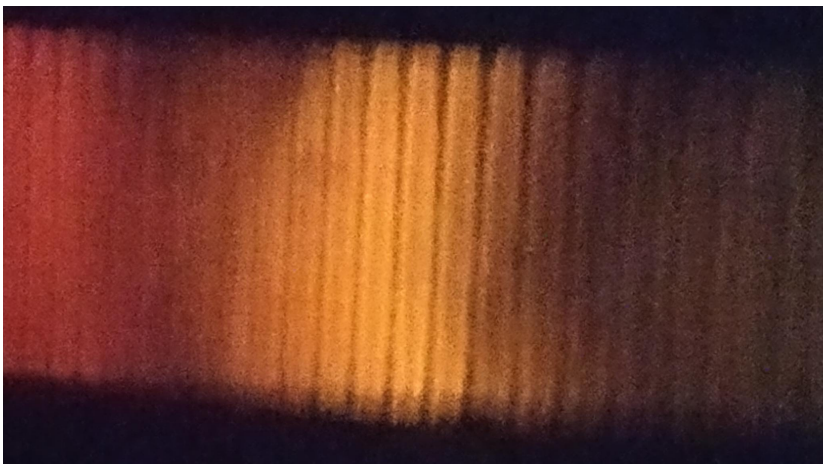

Figure 7: Equidistant pattern observed through the Lummer interferometer at a wavelenght of 603 nm.

λ [nm]	I [A]	H [kG]	J_1	J_2	g_1	g_2	$f(g_1, g_2)$	e/m_e [10^{11} C/kg]
585	1.1 ± 0.1	7 ± 0.5	0	1	0	1.034	$2g_2$	2.0 ± 0.1
588	0.9 ± 0.1	5 ± 0.5	1	2	1.304	1.503	$2g_1$	1.9 ± 0.2
603	1.0 ± 0.1	6 ± 0.5	1	1	1.304	1.464	$2g_1$	1.6 ± 0.1
651	1.1 ± 0.1	7 ± 0.5	2	1	1.137	1.464	$2g_1$	1.8 ± 0.1
653	1.4 ± 0.1	8 ± 0.5	1	0	0.669	0	$2g_1$	2.5 ± 0.1

Table 1: Aquired data from the measurements.

charge mass ratio. This is given by

$$\frac{e}{m_e} = 2\pi c \frac{\Delta\lambda}{\lambda^2 H f(g_1, g_2)}, \tag{42}$$

where a derivation is provided in [2]. The calculated mean value for e/m_e was determined to be $(1.9 \pm 0.1) \cdot 10^{11}$ C/kg, which deviates by 8 % from the literature value [7]. This inaccuracy arises from the fact that the wavelength was determined using Figure 6 and comparing to for example Figure 7. Nevertheless, the literature value lies within the error bound. As Figure 7 shows, the intensity of the lines is not constant throughout the spectral range. It can, therefore, not be excluded that the pattern is not equidistant in the less visible part. However, the uncertainty of 0.1 A does cover this problem, since values deviating more than 0.1 A definitely do not result in a equidistant pattern. Further it shall be noted that the determination of the wavelength was based on an categorisation by eye, where Figure 6 was used as a reference. This has an impact on the calculation as the energy transition in the multiplet structure shown in Figure 8 changes. As a result, this bears a possible source for systematic errors which was indeed the case in this measurement. Overall this experimental setup can be improved in precision and accuracy. In order to achieve higher precision a camera could be mounted at the end of the Lummer interferometer with appropriate resolution. It would then be possible to analyse the pattern with numerical methods. A possibility to achieve higher precision could be done by analysing the wavelength. This could be done by using a lens with focal length at infinity. The resulting beam can then be studied by using a Fabry-Perot-Etalon, ideally with very high finesse, which makes the categorization of the wavelength by eye redundant.

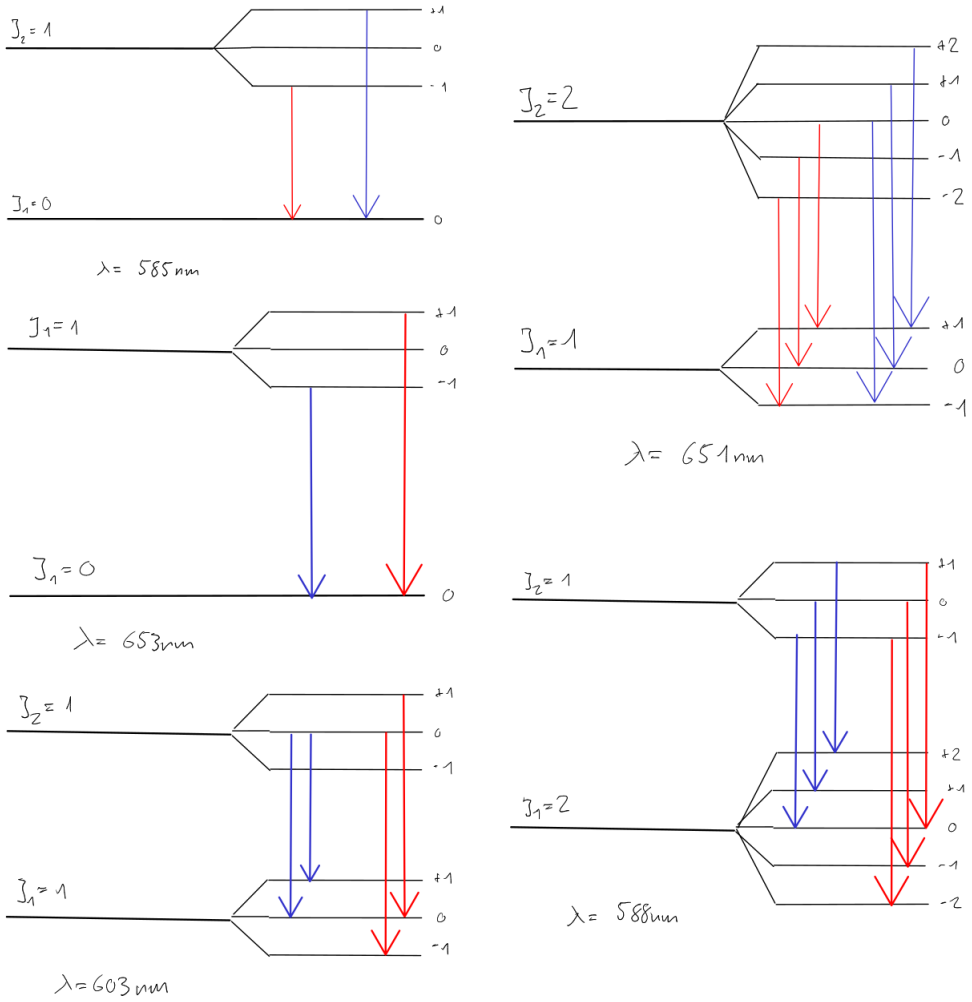

Figure 8: Energy transistion scheme showing the multiplet structure, where transitions with $\Delta m = 0$ are not shown. This arises from the fact that they are not observable with the interferometer.

5 Conclusion

The Zeeman effect could be used to determine the elementary charge mass ratio at $(1.9 \pm 0.1) \cdot 10^{11}$ C/kg, where the literature value deviates by 8 %. The deviation arises from inaccuracy in the determination of the wavelength of the spectral lines and the procedure to find the magnetic field which yields an equidistant pattern. Overall this experiment provides a interesting insight into spectroscopy and the effect of a magnetic field on the emission of light.

References

[1] World Encyclopedia, *Zeeman effect* Oxford University Press, encyclopedia.com (11.12.2019)

[2] ETH VP, *Zeeman Effect Instructions*, ETHZ Physikpraktikum 3+4, vp.phys.ethz.ch/Experimente/pdf/Zeeman.pdf (21.11.2019)

[3] C. Dedes and P. Cerulo, *Franck-Hertz Experiment Instructions*, ETHZ Physikpraktikum 3+4, vp.phys.ethz.ch/Experimente/pdf/Franck_Hertz.pdf (21.11.2019)

[4] The Nobel Prize, *The Nobel Prize in Physics 1902*, nobelprize.org/prizes/physics/1902/ (11.12.2019)

[5] J.P. Home, *Physics III*, ETH Zurich, 1.5.2018

[6] Uncertainties: a Python package for calculations with uncertainties, Eric O. LEBIGOT, http://pythonhosted.org/uncertainties/ (9.11.2019)

[7] Bureau International des Poids et Mesures - SI BASE UNITS, https://www.bipm.org/utils/en/pdf/si-promotion/SI-Base-Units.pdf (22.11.2019)